The AAPS Journal (2019) 21: 3
DOI: 10.1208/s12248-018-0261-2

Research Article

In Vitro and *In Vivo* Efficacy of the Monocarboxylate Transporter 1 Inhibitor AR-C155858 in the Murine 4T1 Breast Cancer Tumor Model

Xiaowen Guan,[1] Mark A. Bryniarski,[1] and Marilyn E. Morris[1,2]

Received 13 May 2018; accepted 30 August 2018; published online 5 November 2018

Abstract. Monocarboxylate transporter 1 (MCT1), also known as a L-lactate transporter, is a potential therapeutic target in cancer. The objectives of this study were to evaluate efficacy and assess concentration-effect relationships of AR-C155858 (a selective and potent MCT1 inhibitor) in murine 4T1 breast cancer cells and in the 4T1 tumor xenograft model. Western blotting of 4T1 cells demonstrated triple negative breast cancer (TNBC) characteristics and overexpression of MCT1 and CD147 (a MCT1 accessory protein), but absence of MCT4 expression. AR-C155858 inhibited the cellular L-lactate uptake and cellular proliferation at low nanomolar potencies (IC_{50} values of 25.0 ± 4.2 and 20.2 ± 0.2 nM, respectively). In the xenograft 4T1 mouse model of immunocompetent animals, AR-C155858 (10 mg/kg i.p. once daily) had no effect on tumor volume and weight. Treatment with AR-C155858 resulted in slightly increased tumor lactate concentrations; however, the changes were not statistically significant. AR-C155858 was well tolerated, as demonstrated by the unchanged body weight and blood lactate concentrations. Average blood and tumor AR-C155858 concentrations (110 ± 22 and 574 ± 245 nM, respectively), 24 h after the last dose, were well above the IC_{50} values. These data indicate that AR-C155858 penetrated 4T1 xenograft tumors and was present at high concentrations but was ineffective in decreasing tumor growth. Evaluations of AR-C155858 in other preclinical models of breast cancer are needed to further assess its efficacy.

KEY WORDS: AR-C155858; breast cancer; monocarboxylate transporter 1 ; 4T1.

INTRODUCTION

Proton-linked lactate transport proteins, also known as monocarboxylate transporters (MCTs), represent the first four members of the SLC16A gene family. MCT1 and MCT4 have been identified as potential new therapeutic targets in cancer due to reports of (1) MCT1 and MCT4 overexpressions correlating significantly with poor prognosis and survival in various types of cancer, including breast cancer and (2) MCT inhibition or MCT silencing resulting in decreased tumor growth in different human cancer xenograft models (1–5). The transport of lactate across the plasma membrane in normal cells requires MCTs 1 through 4, which are involved in the proton-linked facilitated transport of a number of short-chain monocarboxylates (e.g., lactate, pyruvate, ketone bodies) (6–9). In particular, MCT1, MCT4, and CD147 (a chaperone protein required for trafficking and function of MCTs to the plasma membrane) have been reported to be important in cancer (10,11). MCT1 is ubiquitously expressed throughout the body (12), whereas MCT4 is expressed mainly in tissues that are highly glycolytic (6,8). Lactate transport by MCT1 is bidirectional while MCT4 is mainly involved in the efflux of lactate (6,7). The increased rate of glycolysis, a known metabolic phenotype of cancer, results in the production of lactic acid, and thus, the main function of MCTs in glycolytic cells is the transport of lactate along with a proton out of cells to help to sustain the high glycolytic rate and prevent acidosis and apoptosis.

Triple negative breast cancer (TNBC), a highly metastatic and deadly form of breast cancer, remains incurable as it lacks the expression of estrogen receptor (ER) and progesterone receptor (PR), and lacks human epidermal growth factor receptor 2 (HER2) amplification. With breast cancer being a highly heterogeneous disease, the classification of clinically defined TNBC consists of multiple and diverse subclasses (13). Although a number of therapeutic targets have been identified, there has not been a proven targeted therapy available for patients with this form of breast cancer.

[1] Department of Pharmaceutical Sciences, School of Pharmacy and Pharmaceutical Sciences, University at Buffalo, State University of New York, 352 Kapoor Hall, Buffalo, New York 14214, USA.
[2] To whom correspondence should be addressed. (e-mail: memorris@buffalo.edu)

Abbreviations MCTs, Monocarboxylate transporters; TNBC, Triple negative breast cancer; CD147, Basigin; ER, Estrogen receptor; PR, Progesterone receptor; HER2, Human epidermal growth factor receptor 2; GHB, Gamma-hydroxybutyric acid

Recent studies have reported that overexpression of MCT1 and CD147 protein expression correlated significantly with poor histological parameters of basal-like breast cancer categorized as TNBC (14,15), suggesting the potential role of MCT1 in TNBC.

AR-C155858 (6-[(3,5-dimethyl-1H-pyrazol-4-yl)methyl]-5-[(4S)-4-hydroxy-1,2-oxazolidine-2-carbonyl]-3-methyl-1-(2-methylpropyl)thienol[2,3-d]pyrimidine-2,4-dione) is a member of a new class of potent and selective inhibitors of MCT1 developed by AstraZeneca (Fig. 1) (16). The analogue of AR-C155858, AZD3965, is currently in a phase I clinical trial in the UK for solid tumors and lymphomas (NCT01791595). Unlike the classical inhibitors of MCT, the potency of AR-C155858 and AZD3965 is in the low nanomolar range and the selectivity is highly specific to MCT1, with lower affinity for MCT2, and no inhibition of MCT4 (3,17–19). The proposed mechanism of inhibition by AR-C155858 involved binding from the intracellular side of MCT1 (18). *In vitro* and *in vivo* anticancer activities of AR-C155858 have been demonstrated in multiple myeloma cells (20), pancreatic ductal adenocarcinoma cells (5), breast cancer cells (21,22), and in xenograft models of Ras-transformed fibroblasts (23) and Raji lymphoma (21). To date, very few studies have evaluated the effect of MCT1 inhibition in breast cancer, although AR-C155858 has been reported to inhibit lactate export and cell growth in MCF7 breast cancer cells, an ER-positive breast cancer model (21,22).

The murine 4T1 breast tumor xenograft model is an animal model for stage IV human breast cancer and it represents one of the few preclinical breast cancer models available that closely mimics the metastatic phenotype of human breast cancer with similar TNBC characteristics. (24–27). The characterization of 4T1 breast cancer model has been considered to be, and used as, a TNBC model (25,28). In this study, we characterized the 4T1 breast cancer cell line and demonstrated protein expression of MCT1 and CD147 but not MCT4 in this cell line. The goals of present research were to evaluate the *in vitro* and *in vivo* efficacy of AR-C155858 and assess the concentration-effect relationships of AR-C155858 in the murine 4T1 breast cancer model.

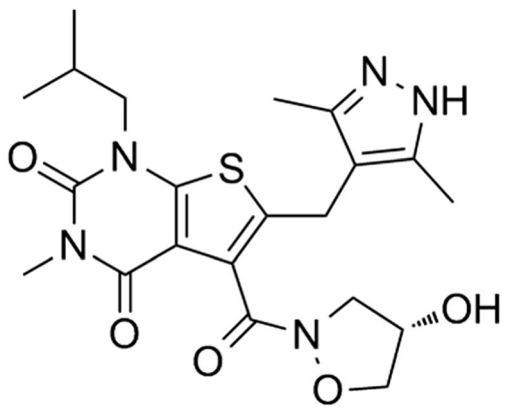

Fig. 1. Chemical structure of AR-C155858 (6-[(3,5-dimethyl-1H-pyrazol-4-yl)methyl]-5-[(4S)-4-hydroxy-1,2-oxazolidine-2-carbonyl]-3-methyl-1-(2-methylpropyl)thienol[2,3-d]pyrimidine-2,4-dione)

MATERIALS AND METHODS

Chemicals and Reagents

L-Lactate (as calcium salt) was purchased from Sigma-Aldrich (St. Louis, MO). AR-C155858 was purchased from ChemScene (Monmouth Junction, NJ). L-[^{3}H] Lactate was purchased from American Radiolabeled Chemicals (St. Louis, MO).

Cell Culture

Mouse mammary tumor, 4T1, and mouse mammary epithelial NMuMG cells were kindly provided by Dr. Elizabeth A. Repasky (Roswell Park Cancer Institute, Buffalo, NY) and Dr. Karen J.L. Burg (University of Clemson, SC), respectively. Cells were maintained at 37°C in a humidified atmosphere with 5% CO_2/ 95% air. 4T1 cells were cultured in RPMI 1640 medium supplemented with 10% FBS, 100 units penicillin, and 100 μg/ml of streptomycin. NMuMG cells were cultured in DME medium supplemented with 10 μg/ml of insulin, 10% FBS, 100 units penicillin, and 100 μg/ml of streptomycin. Culture medium was changed every 2–3 days, and cells were passaged with 0.25% trypsin/EDTA.

Western Blotting Analysis

Total plasma membrane protein was isolated using ultracentrifugation, according to the protocol by Zhang *et al.* (29). For total protein extraction, cells were harvested and lysed in RIPA lysis buffer supplemented with protease inhibitor on ice for 30 min and then centrifuged at 16,000×*g* for 20 min at 4°C. The resulting supernatants were collected for western blot. Membrane protein and total protein samples were denatured in Laemmli loading buffer at 37°C for 30 min or 95°C for 5 min, respectively. Twenty micrograms of the protein was run per lane in 10% SDS-PAGE gel and transferred electrophoretically onto nitrocellulose membranes (Bio-Rad, Hercules, CA). Membranes were blocked with 5% (*w*/*v*) nonfat milk in Tris or phosphate buffered saline containing 0.05% (*v*/*v*) Tween 20 overnight at 4°C. Selective antibodies against MCT1 (1:5000; ab3538P, EMD Millipore), MCT4 (1:500; sc50329, Santa Cruz), CD147 (1:100; sc9757, Santa Cruz), ER (1:1000; ab32063, EMD Millipore), PR (1: 1000; ab131486, EMD Millipore), and HER2 (1:1000; 2165, Cell Signal) were used to blot the membranes for 4 h at 20°C or overnight at 4°C, followed by incubation with secondary antibody coupled to horseradish peroxidase (HRP) for 1 h at 20°C. Na^+K^+ ATPase (1:500; sc71638, Santa Cruz) and GAPDH (1:5000; sc25778, Santa Cruz) were used as loading control for membrane and total protein, respectively. Membranes were incubated with ECL substrates for 5 min followed by visualization in ChemiDocTM XRS + system (Bio-Rad, Hercules, CA).

Cellular Uptake Studies

The concentration dependent inhibition of L-lactate uptake by AR-C155858 was evaluated in 4T1 cells. In brief,

4T1 cells were plated in 35 mm (diameter) culture dishes at a cell density of 2.0×10^5 cells/ml 2 days before the uptake study. On the day of the study, culture medium was removed and cells were washed three times followed by equilibration for 20 min at 37°C in the sodium-free uptake buffer containing 137 mM *N*-methyl-D-glucamine, 5.4 mM KCl, 1 mM $CaCl_2$, 1 mM $MgCl_2$, and 10 mM HEPES (pH 6.0). Cells were preincubated with various concentrations of AR-C155858 for 30 min at 37°C and allowed to cool to room temperature for 5 min. Cells then were incubated in 1 ml of uptake buffer containing [^{3}H]-L-lactate (0.5 mM) and uptake determined for 1 min. Time-dependent uptake studies had determined that there was linear uptake over this time frame. For time-dependent uptake, cells were incubated with uptake buffer containing 1 μCi of [^{3}H]-L-lactate for 0.5, 1, 5, 10, 15, 30, 60, and 120 min. To determine the concentration-dependent uptake of L-lactate, L-lactate concentration ranged from 0 to 70 mM. The uptake was terminated by aspirating the uptake buffer, and the cells were washed immediately three times with ice-cold buffer. Cells were lysed in 0.5 ml of 1.0 N NaOH for 1 h at room temperature, and the cell lysates were neutralized with 0.5 ml of 1.0 N HCl. Three milliliters of scintillation fluid was added to 400 μl of cell lysate and the radioactivity was determined by liquid scintillation counting (1900 CA, Tri-carb liquid scintillation analyzer, Packard Instrument Co., Downers Grove, IL). Protein concentrations were determined using a bicinchoninic acid protein assay kit (BCA, Pierce Chemicals, Rockford, IL). All the results were normalized to total protein content and were expressed as picomoles or nanomoles per milligram of protein.

Cell Proliferation Studies

4T1 cells were plated in 96-well plates at a cell density of 5.0×10^3 cells per well in 100 μl of complete medium and allowed to adhere overnight. On the day of the study, the medium was removed and cells were washed with 1× PBS. Cells were treated with various concentrations of AR-C155858 in 100 μl of serum free medium for 48 h. Relative cell growth was quantified using Cell Proliferation Reagent WST-1 (Roche Applied Science), according to the manufacturer's instructions. The results were normalized to the vehicle control (< 0.1% DMSO) and expressed as percentage of cell growth.

Animals

Female, BALB/c mice, 5 to 6 weeks of age (18–20 g), were obtained from Envigo (Indianapolis, IN). Mice were housed in a filtered laminar airflow room in standard vinyl cages. Water and food were provided *ad libitum*. Animals were maintained under the standard 12 light/dark cycle at 22–24°C. All animal protocols were approved by the Institutional Animal Care and Use Committee at the University at Buffalo.

In Vivo Tumor Growth Experiments

After 2 weeks of acclimatization, mice were lightly anesthetized and injected with 100 μl of cell suspension subcutaneously into the 4th inguinal mammary fat pad at a cell density of 2.5×10^5 cells/ml in 1× PBS, as previously described (30). Prior to inoculation, 4T1 cells were treated with trypsin, washed and resuspended in 1× PBS. One day after tumor inoculation, animals were randomly divided into two treatment groups (five mice per group): (i) vehicle control and (ii) AR-C155858 (10 mg/kg). This treatment schedule was used to model the clinical situation when spontaneous metastases are not present. This treatment has no interference with the 4T1 tumor engraftment, as previously reported (31). AR-C155858 stock solution (2 mg/ml) was prepared in vehicle control, which consisted of 10% *w*/*v* cyclodextrin in normal saline (32). AR-C155858 or vehicle was administered once daily, intraperitoneally (i.p.) for 28 days. Throughout the study, body weights were monitored weekly and tumor volumes were measured every 2–3 days using a digital caliper. Tumor volumes were calculated with Eq. 1.

$$\text{Tumor volume} = \frac{\text{Length} \times \text{Width}^2}{2} \quad (1)$$

At the end of the study, blood samples were collected from the aortic artery. Primary tumor samples were collected and snapped frozen in liquid nitrogen. All samples were stored at − 80°C until analysis.

l-Lactate Assay

Blood and tumor lactate concentrations were measured by a colorimetric assay (Eton Biosciences, Inc., Union, NJ) based on a standard curve of known lactate concentrations. Prior to performing the assay, samples were deproteinized using 10 kDa molecular weight cutoff spin columns. For quantifying intratumor lactate concentrations, tumor samples were thawed on ice and homogenized in 1× PBS (8 ml/g tumor). Tumor homogenates were incubated with gentle rolling motion for 1 h at 4°C and centrifuged at 10,000×*g* for 10 min. The resulting supernatants were collected for the lactate assay. Intratumor lactate concentrations were normalized to gram of tumor tissue.

Blood and Tumor Sample Preparation and LC/MS/MS Analysis

AR-C155858 blood and tumor concentrations were measured using a previously developed and validated liquid chromatography coupled to tandem mass spectrometry (LC/MS/MS) assay (30). For tumor samples, tumors were thawed on ice and homogenized in methanol/water (5/95, *v*/*v*), (5 ml/g tumor). Briefly, samples were prepared by adding 5 μl of the internal standard (I.S.) AZD3965 (8 ng/ml) to 55 μl of blood or tumor homogenate samples. Standards and quality controls were prepared by adding 5 μl of I.S. and 5 μl of AR-C155858 stock solutions to 50 μl of blank blood or tumor homogenate. Blood and tumor proteins were precipitated by the addition of 600 μl 0.1% formic acid in acetonitrile. Samples were vortexed, followed by centrifugation at 10,000×*g* for 20 min at 4°C. Then, 540 μl of the supernatant

was collected and evaporated under a stream of nitrogen gas, followed by reconstitution in 200 μl of acetonitrile/water (40/60, *v*/*v*).

The LC/MS/MS assay was validated in blood and tumor tissues using a Shimadzu Prominence HPLC with binary pump and autosampler (Shimadzu Scientific, Marlborough, MA) connected to a Sciex API 3000 triple quadruple tandem mass spectrometer with an Atmospheric Pressure Chemical Ionization source (APCI) (Sciex, Foster City, CA). Chromatographic separation was achieved by injecting 15 μl of the sample on to an Xterra MS C18 column (250 × 2.1 mm i.d., 5-μm particle size; Waters, Milford, MA). Mobile phase A consisted of acetonitrile/water (5/95, *v*/*v*) with 0.1% acetic acid, and mobile phase B was acetonitrile/water (95/5, *v*/*v*) with 0.1% acetic acid. The flow rate was 250 μl/min with a gradient elution profile and a total run time of 15 min. The mass spectrometer was operated in multiple reaction monitoring (MRM) mode utilizing an APCI source. *Q*1/*Q*3 *m*/*z* ratio for the precursor/product ion of AR-C155858 and AZD3965 was 462.3/373.2 and 516.4/413.2, respectively. The data was analyzed using Analyst version 1.4.2 (Sciex, Foster City, CA).

Regression analysis of peak area ratios of AR-C155858/AZD3965 to AR-C155858 concentrations was used to assess linearity of the curve. The intraday and inter-day precision and accuracy were determined using quality control (*QC*) samples at 2 ng/ml (low *QC*), 30 ng/ml (medium *QC*), and 70 ng/ml (high *QC*). For the intraday precision and accuracy, quality control samples were analyzed in triplicate on each day, whereas for the inter-day precision and accuracy, quality control samples were analyzed over three different days. A calibration curve was run on each analysis day along with the quality controls, and the curve was analyzed by the ratio of the peak area of AR-C155858 and AZD3965 with $1/\chi$ weighted least squares linear regression analysis (χ = concentration). The precision was determined by the coefficient of variation, and accuracy was measured by comparing the calculated concentration with the known concentration. The acceptable precision and accuracy were within ± 15%.

Data Analysis

All the data are presented as mean ± SD. Data analysis was performed using GraphPad Prism (GraphPad Software Inc., San Diego CA). Depending on the number of groups and variances, data were compared with Student's *t* test or two-way ANOVA followed with Bonferroni's post-hoc comparisons. Significant differences were based on the criterion $P < 0.05$. The transport kinetic parameters: Michaelis-Menten constant K_m, maximal velocity V_{max}, and diffusional clearance P were determined using the following equations:

$$\mathcal{V} = \frac{V_{max} \times C_{L\text{–}lactate}}{K_m + C_{L\text{–}lactate}} \tag{2}$$

$$\mathcal{V} = \frac{V_{max} \times C_{L\text{–}lactate}}{K_m + C_{L\text{–}lactate}} + P \times C_{L\text{–}lactate} \tag{3}$$

where v is the rate of L-lactate uptake and $C_{L\text{-}lactate}$ is the concentration of L-lactate. The inhibition of L-lactate uptake and cell growth by AR-C155858 (IC_{50}) was calculated using the equation below:

$$R = R_0\left(1 - \frac{I_{max} \times C^{\gamma}}{IC_{50}{}^{\gamma} + C^{\gamma}}\right) \tag{4}$$

where R and R_0 are the percentage of L-lactate uptake or cell growth in the presence and absence of the inhibitor, respectively. C is the concentration of the inhibitor. I_{max} is the maximal inhibition, γ is the Hill coefficient, and IC_{50} is the concentration of the inhibitor at half maximal inhibition. IC_{50} was estimated using weighted nonlinear regression analysis (ADAPT 5 Biomedical Simulations Resource (BMSR), University of South California, Los Angeles, CA).

RESULTS

Characterization of 4T1 Breast Cancer Cells

4T1 murine breast tumor cells were evaluated for TNBC characteristics; western blotting demonstrated little ER (Fig. 2a) and negligible PR (Fig. 2b) expression and no overexpression of HER2 (Fig. 2c) in the 4T1 cells. The lack of PR and ER expression in NMuMG cells was used as a negative control. The plasma membrane protein expression of MCT1, MCT4, and CD147 was characterized in 4T1 cells. 4T1 cells demonstrated expression of MCT1 (Fig. 2d), CD147 (Fig. 2e), and no expression of MCT4 (Fig. 2f). The expression of MCT1 in 4T1 cells was comparable to that present in KNRK cells, which is a rat kidney cell line that we had previously shown to express MCT1 (data not shown). Interestingly, NMuMG cells expressed appreciable amounts of MCT4 (Fig. 1e). The expression of MCT2 was weakly present on the plasma membrane of 4T1 cells (data not shown).

Kinetics of *l*-Lactate Uptake in 4T1 Cells

The time-dependent uptake of L-lactate by 4T1 cells was linear up to 15 min (Fig. 3a), and a 1 min uptake time was chosen for the uptake studies to minimize loss due to metabolism (33). L-Lactate uptake in 4T1 cells exhibited pH (determined at pH 6.0 and 7.4, data not shown) and concentration dependence (Fig. 3b). The concentration-dependent uptake of L-lactate at pH 6.0 demonstrated saturable uptake, and its uptake was best described by Eq. 3 with a K_m of 3.88 ± 0.86 mM, V_{max} of 414 ± 58 nmol/mg/min and diffusional clearance of 12.0 ± 1.3 μl/mg/min (Table I; Fig. 3b). From these studies, an optimized condition with 1 min uptake time and 0.5 mM L-lactate was used to evaluate the effect of AR-C155858 on cellular uptake of L-lactate.

In Vitro Effect of AR-C155858 on *l*-Lactate Uptake and Cell Growth

Concentration-dependent inhibition of L-lactate uptake (Fig. 4a) and cell growth (a relative measurement based on the WST-1 assay) (Fig. 4b) by AR-C155858 was

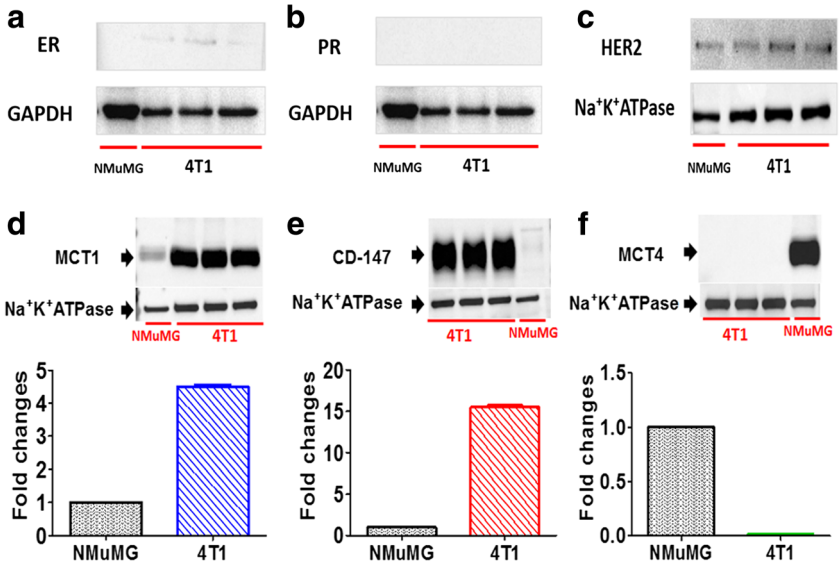

Fig. 2. Characterization of the murine 4T1 breast tumor model. The murine 4T1 breast tumor model exhibited similar TNBC characteristics as in human TNBC. Presented are cytosolic ER (**a**) and PR (**b**) expressions, plasma membrane expression of HER2 (**c**), plasma membrane protein expression of MCT1 (**d**), and CD147 (**e**) and MCT4 (**f**) proteins in 4T1 cells relative to murine mammary epithelial cells (NMuMG). Histograms show corresponding densitometry analysis of the membranes from western blots of MCT1, MCT4, and CD147 (20 μg per lane). GAPDH and Na^+K^+ ATPase were used as loading controls for total and membrane protein, respectively

demonstrated, and the IC_{50} values were found to be 25.0 and 20.2 nM, respectively (Table II).

Blood and Tumor ARC155858 Quantification by LCMS/MS

From the mouse blood and tumor AR-C155858 LC/MS/MS assays, the lower limit of quantification for AR-C155858 was found to be 0.1 ng/ml with high precision and accuracy. The standard curve range for AR-C155858 was from 0.1 to 100 ng/ml, based on regression analysis of peak areas to AR-C155858 concentrations ($r^2 > 0.999$). The intraday and inter-day precision and accuracy of the quality control samples are summarized in Table III.

In Vivo Efficacy of AR-C155858 in the 4T1 Breast Tumor Xenograft

Groups of five mice inoculated with 4T1 tumor cells were treated with 10 mg/kg AR-C155858 or vehicle control once a day (i.p.) for 28 days, starting 1 day after tumor implantation (Fig. 5a). This treatment approach was used to imitate the clinical situation prior to the presence of metastases. AR-C155858 treatment did not significantly alter the body weight monitored throughout the study (Fig. 5b). Treatment with AR-C155858 had no effect on tumor volume (Fig. 5c) nor was there a decrease in the primary tumor weight (Fig. 5d). Further analysis of blood and tumor lactate concentration revealed that the tumor

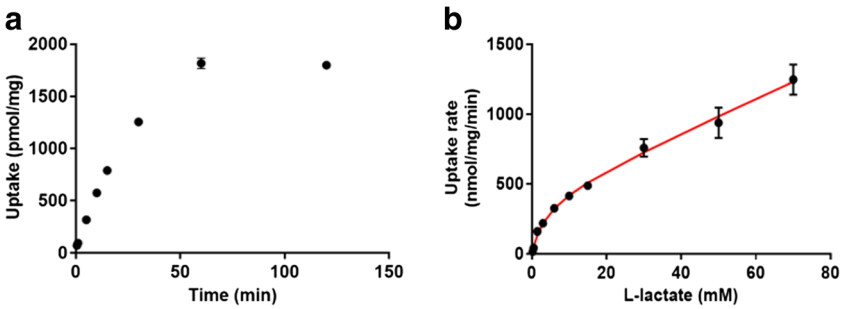

Fig. 3. L-Lactate uptake kinetics in 4T1 cells. Presented is the time-dependent L-lactate uptake at pH 6.0 (**a**), and concentration-dependent uptake of L-lactate at pH 6.0 (**b**). The concentration-dependent data were best fitted to a Michaelis-Menten equation with diffusional uptake clearance component (P). Observed mean data from three studies are shown (symbols), with the line representing the model-fitted results

Table I. Cellular L-Lactate Uptake Kinetic Parameter Estimates in 4T1 Cells. $n = 3$

Parameter	Mean ± SD	CV%
V_{max} (nmol/mg/min)	414 ± 58	14.1
K_m (mM)	3.88 ± 0.86	22.2
P (μl/mg/min)	12.0 ± 1.3	11.2

lactate concentrations were not significantly elevated with AR-C155858 treatment when compared to the vehicle control (Fig. 5e; Table IV), and the treatment did not alter blood lactate concentrations significantly (Fig. 5f; Table IV). Extensive tumor necrosis was observed in both vehicle- and AR-C155858-treated tumors (Fig. 5g). The blood and total tumor AR-C155858 concentrations were investigated when the mice were sacrificed on day 29 (24 h after the last AR-C155858 dose). Total tumor AR-C155858 concentration (574 ± 245 nM) was found to be 5-fold higher than that in the blood (110 ± 22 nM), suggesting that there was extensive accumulation of AR-C155858 in the 4T1 tumor (Fig. 6).

DISCUSSION

Overexpression of MCT1 in human TNBC, compared to normal breast tissue, has been reported to correlate with poor clinical outcome (14,15), but very few studies have evaluated the effect of MCT1 inhibition in breast cancer (21,22). AR-C155858 has been demonstrated to inhibit growth in estrogen-positive MCF-7 cells that express both MCT1 and MCT4, and an analogue of AR-C155858 (AR-C12298) has been reported to inhibit tumor growth in a MCF-7 xenograft animal model (21,22). In our present study, we have utilized a murine 4T1 breast tumor model (considered as a TNBC model), which expresses only MCT1, to evaluate the efficacy of AR-C155858 *in vitro* and *in vivo*.

The murine 4T1 breast tumor model represents a late-stage breast cancer model that has shown to exhibit a similar phenotype as human TNBC. Our data are consistent with the results of a previous immunohistochemical analysis by Bao *et al.* (25), demonstrating TNBC characteristics in the 4T1 cells. The lack of PR and ER expression in the NMuMG cell line, which was used as the negative control, was also in line with what was reported previously (34). Similar to previous studies, our results demonstrated expression of MCT1 and CD147 and absence of MCT4 on the plasma membrane of 4T1 cells, indicating that the 4T1 breast tumor cell line is a relevant model for studying the effect of MCT1 inhibition (35).

AR-C155858, a pyrrole pyrimidine derivative, is a member of a new and potent class of MCT1 inhibitors. Its K_i value is approximately 2.3 nM in rat erythrocytes, which express only MCT1 (18). AR-C155858 has been shown to have some inhibitory activity against MCT2 but it does not inhibit MCT4 (18,19). The low nanomolar potency of AR-C155858 from our cellular L-lactate uptake and cell growth studies was consistent with the IC_{50} value determined previously for the inhibition of uptake of gamma-hydroxybutyric acid (GHB), another MCT1 substrate, in the rat kidney KNRK cell line that expresses MCT1 (32).

We observed that blocking MCT1 activity by AR-C155858 resulted in potent inhibition of 4T1 cell growth based on a relative proliferative assay, with an IC_{50} value of 20.3 nM. Payen *et al.* indicated no effect on cell numbers at a concentration of 10 nM; additionally, there were no changes in migration and invasion at this concentration, although there were significant reductions in glucose consumption and lactate efflux (35). However, these authors reported that knocking down MCT1 via shRNA or deleting MCT1 via CRISPR in 4T1 cells resulted in a reduction in cell migration and invasion (35). Additionally, in SiHa-F3 cells (human cervix adenocarcinoma cells) that express both MCT1 and MCT4, there was no effect on cell migration and invasion, even at a much higher concentration of AR-C155858 (10 μM) that inhibited lactate efflux but not glucose consumption (35). In the SiHa-F3 cell study, the authors verified that AR-C155858 treatment did not alter MCT and CD147 expression in the cells. Other studies have reported that AR-C155858 (at a high concentration of 10 μM) had no effect on cell migration but affected cell invasion

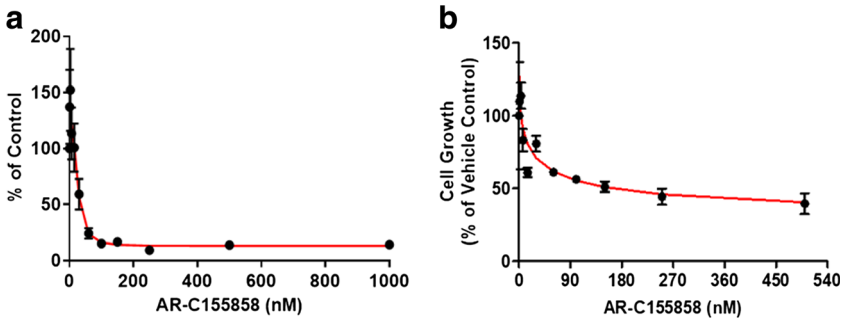

Fig. 4. Effect of AR-C155858 on L-lactate uptake and cell growth in 4T1 cells. Inhibition of radiolabeled L-lactate (0.5 mM) uptake at pH 6.0 by AR-C155858 (**a**). Percentage of cell growth after 48 h of AR-C155858 treatment with results normalized to vehicle control-treated cells (**b**). Observed mean data from three studies are shown (symbols), with the line representing model fitting results

Table II. IC_{50} Estimates of AR-C155858 in Cellular L-Lactate Uptake (pH 6.0) and Cell Growth Studies (Physiological pH). $n = 3$

	Mean ± SD (nM)	CV%
Cellular L-lactate uptake	25.0 ± 4.2	16.9
Cell growth	20.3 ± 0.2	47.6

in pancreatic ductal adenocarcinoma cells (PDAC), specifically the BXpC3 cell line that expresses both MCT1 and MCT4 (5). No effects on cell invasion in other PDAC cell lines were found (5), indicating that the effect may be cell line specific. Therefore, varying concentration- and cell-dependent effects of AR-C155858 on cell proliferation, migration, and invasion have been reported.

The effect of AR-C155858 (100 nM) on cell death has been reported in MCF7 breast cancer and Raji lymphoma cells (21). However, in our study, AR-C155858 demonstrated marginal effects on cell death at 3 nM in 4T1 cells where the extent of cell death was measured based on the histone-associated DNA fragment activity (unpublished data). Although the discrepancy could likely be due to the *in vitro* system used and the type of measurement used to quantitate cell death, studies with AZD3965 (8 nM) showed minimal apoptotic cell death, as quantitated by evaluating the total keratin (CK) 18 and cleaved caspase 3. In COR-L103 cells of small cell lung carcinoma that express only MCT1, Polanski *et al.* showed that AZD3965 treatment resulted in the accumulation of CK18 in the media but not the caspase cleaved form of CK18, supporting the hypothesis that cell death mediated by AZD3965 is nonapoptotic (2). From those studies, Polanski *et al.* showed that AZD3965 induced a nonapoptotic and autophagic form of cell death and proposed that AZD3965 is likely involved in necrotic cell death (2). Further investigations are needed to better understand the effect of AR-C155858 on cell death, as the effect could also likely be compound specific.

Our laboratory has shown previously that at a much lower dose, 1 mg/kg i.v., AR-C155858 significantly inhibited MCT1-mediated transport of the substrate GHB, as demonstrated by a reduction in GHB plasma concentrations and increase in MCT-mediated renal clearance (32). A higher dose of AR-C155858, 5 mg/kg, did not produce additional changes in GHB pharmacokinetics (32). The effect of AR-C155858 was dose-dependent from 0.1 to 1 mg/kg (32). In those studies, AR-C155858 treatment resulted in a significant decrease in GHB brain/plasma ratio at steady state (32); MCT1 is the only isoform expressed at the blood-brain barrier and is responsible for the uptake of GHB into the brain (36–39). Based on our previously published pharmacokinetic data in rats (16,32) demonstrating a long half-life, and our dose-effect relationships using GHB as a substrate, a dose of AR-C155858 of 10 mg/kg i.p. once daily was chosen to achieve concentrations above the IC_{50}. To verify that we are achieving concentrations above the IC_{50} for lactate cellular uptake inhibition, we quantified AR-C155858 blood and tumor trough concentrations, 24 h after the last dose. When corrected for protein binding, 66% in rat plasma (16), the free trough AR-C155858 concentrations (37.4 ± 7.58 nM) remain above the *in vitro* effective concentration, indicating that the AR-C155858 dosing regimen produces concentrations above the unbound IC_{50} value throughout the dosing regimen. The tumor AR-C155858 concentration was five times higher than that observed in blood indicating extensive accumulation and uptake of AR-C155858 in the tumor tissue.

With this dosing regimen given over 28 days, AR-C155858 had no effect on the body weight and blood lactate concentrations, and no effect on the tumor volume and weight. Although we were not able to evaluate MCT1 and MCT4 expression in tumors over time in this study, we have seen no significant changes in MCT1 or MCT4 expression in untreated 4T1 xenograft mice over a 17-day treatment period (unpublished data).

Since inhibiting MCT1 efflux is expected to result in the intracellular lactate accumulation, thereby limiting the survival of cancer cells, we also investigated the effect of AR-C155858 on tumor lactate concentration. We did not observe a significant increase in the tumor lactate concentration in animals treated with AR-C155858, although there was a trend towards higher tumor lactate concentrations. We also observed extensive tumor necrosis and lung macrometastases (data not shown) in both control- and

Table III. AR-C155858 Intraday and Inter-day Accuracy and Precision in Mouse Blood and Tumor. The measured concentrations represent mean of triplicate measurement. The analysis was performed over 3 days

Matrix	Nominal concentration (ng/ml)	Intraday				Inter-day			
		Mean (ng/ml)	SD	Precision (CV%)	Accuracy (%)	Mean (ng/ml)	SD	Precision (CV%)	Accuracy (%)
Blood	2	1.60	0.07	4.38	80.0	1.57	0.06	3.90	78.5
	30	26.9	0.3	1.12	89.7	25.5	1.1	4.26	85.0
	70	58.5	1.4	2.37	83.6	55.3	3.4	6.14	79.1
Tumor	2	1.86	0.02	1.12	92.8	1.86	0.01	0.36	92.8
	30	26.8	0.6	2.28	89.4	26.8	0.2	0.83	89.3
	70	64.4	1.1	1.66	92.0	62.8	1.5	2.36	89.8

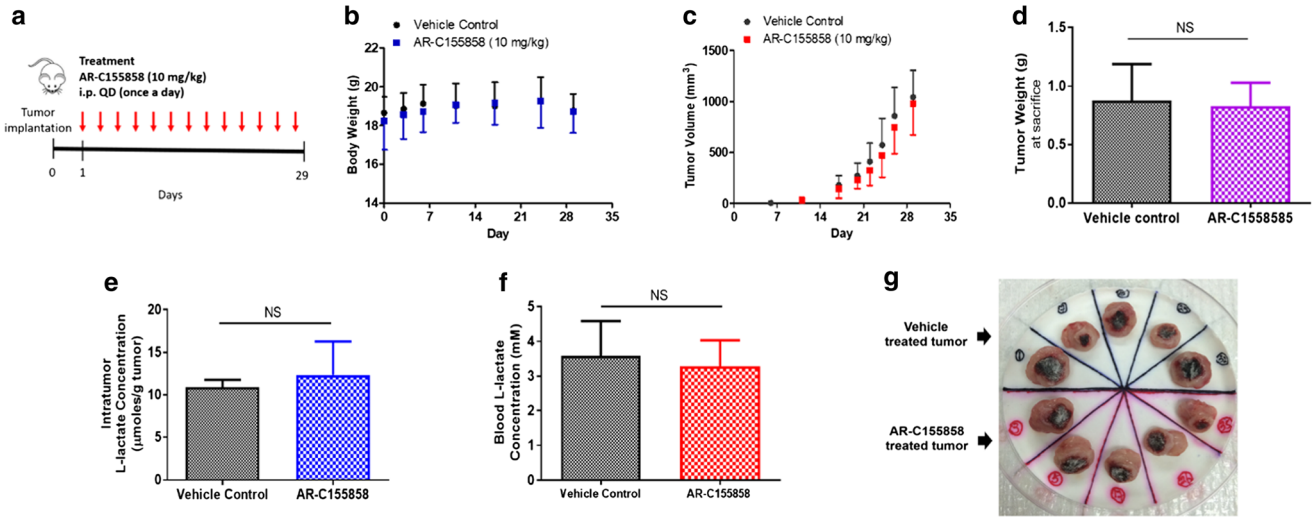

Fig. 5. *In vivo* efficacy of AR-C155858 in the 4T1 breast tumor xenograft. A schematic representation of the experimental timeline and dosing schedule following orthotopic inoculation of 4T1 cells subcutaneously into the mammary fat pad of female BALB/c mice. Mice were given i.p. injection of AR-C155858 (10 mg/kg) or vehicle control once a day (**a**). Body weight (**b**) and tumor volume (**c**) were monitored throughout the study. Tumor weight (**d**), intratumor (**e**), and blood (**f**) lactate concentration were measured at the end of the treatment. Primary tumor excised at the end of the study showed tumor necrosis in both vehicle- and AR-C155858-treated tumors (**g**). All the data are presented as mean ± SD, $n = 5$ in each group. NS nonsignificant, $P > 0.05$ compared to the vehicle control-treated group (two-way ANOVA followed by Bonferroni's post-hoc test or nonparametric Student's *t* test)

AR-C155858-treated animals. Our results contrast with those of a recent study by Payen *et al.* which showed that knocking down MCT1 via shRNA in 4T1 cells profoundly decreased lung metastasis in the 4T1 breast tumor xenograft model when the tumor cells were subcutaneously implanted to the flank of the animals (35). However, Payen *et al.* also reported that AR-C155858 also did not alter migration and invasion of 4T1 cells *in vitro*.

Although knockdown of MCT1 alone or along with MCT4 has been reported to delay tumor growth in human breast cancer cell line-derived xenografts expressing MCT1 and/or MCT4 (4), to our knowledge, there is only one report examining the *in vivo* effect of AR-C155858 in a Ras-transformed fibroblast xenograft model expressing MCT1 (23). In that study, AR-C155858 was given subcutaneously at 30 mg/kg, once daily over 6 days, and it significantly delayed tumor growth (23). Although we demonstrated extensive tumor uptake and accumulation of AR-C155858 at a dose of 10 mg/kg i.p., AR-C155858 was not effective in inhibiting tumor growth in the 4T1 breast tumor animal model in this study. The *in vivo* effect of AR-C155858 in the 4T1 immune competent murine model has not been previously studied, and our investigation is the first report that evaluated plasma and tumor concentrations of AR-C155858. Although we did not evaluate the effect of AR-C155858 on immune function in our study, we have demonstrated immunosuppressive effects of an AR-C155858 analogue, AZD3965, in animals bearing the 4T1 tumor (unpublished data), suggesting that the effect of this pyrrole pyrimidine derivative class of MCT1 inhibitors on immune function may have impacted the overall antitumor efficacy of AR-C155858. Additionally, reduction in spleen weight in animals treated with AZD3965 has been recently been reported in a human Burkitt's lymphoma cell line (CA46)

Table IV. Tumor and Blood L-Lactate Concentration in Animals Treated with Vehicle Control and AR-C155858 (10 mg/kg, i.p., Once Daily). Samples were obtained 24 h after the last AR-C155858 dose. Mean ± SD (Fold change relative to vehicle control) $n = 5$

	Vehicle control	AR-C155858
Blood (mM)	3.59 ± 0.89	3.27 ± 0.68 (0.91)
Tumor (µmol/g tumor)	10.9 ± 0.8	12.4 ± 4.0 (1.1)

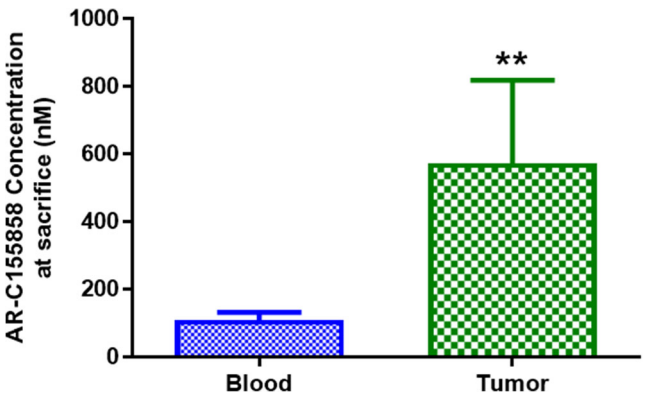

Fig. 6. Blood and total tumor AR-C155858 concentrations measured at the end of the treatment (24 h after the last AR-C155858 dose). Assuming tumor density of 1 g/cm^3, tumor AR-C155858 concentrations were normalized to gram of tumor tissue and expressed in nanomolar. All the data are presented as mean ± SD, $n = 5$. $^{**}P < 0.01$, compared to the blood AR-C155858 concentration (nonparametric Student's *t* test)

derived xenograft in severely immunocompromised NSG mice (1). Taken together our data suggest that differences in efficacy may be dependent on the preclinical xenograft model used, including the use of immunosuppressed *versus* immunocompetent animal models. It is also possible that MCT1 may induce metastasis independent of its transport function, as suggested by Payen *et al.* (35), resulting in differences with complete MCT1 knockdown *versus* chemical inhibition.

CONCLUSION

In summary, our study demonstrated potency of AR-C155858 in inhibiting cellular L-lactate uptake and cell growth in the murine 4T1 cell line (considered as a TNBC model); however, *in vivo* AR-C155858 treatment was ineffective in the murine 4T1 xenograft breast tumor model. Assessment of concentration-effect relationships of AR-C155858 suggests that the lack of efficacy of AR-C155858 is not likely due to low tumor concentrations, since tumor concentrations were above the IC_{50} concentrations for lactate uptake and cell proliferation determined *in vitro*. Our present study indicates that further studies in other preclinical models, with other dosing regimens, and potentially in combination with other chemotherapeutic agents, are needed to provide insight into the therapeutic efficacy of the MCT1 inhibitor AR-C155858 in TNBC.

ACKNOWLEDGMENTS

We thank Donna Ruszaj for her assistance in the LC/MS/MS.

AUTHORS' CONTRIBUTIONS

Participated in research design: Guan and Morris
Conducted experiments: Guan and Bryniarski
Contributed new reagents or analytic tools: Guan and Morris
Performed data analysis: Guan and Morris
Wrote or contributed to the writing of the manuscript: Guan and Morris

FUNDING

This work was funded by the National Institute of Health National Institute on Drug Abuse (grant DA023223). X.G. was funded in part by Allen Barnett Fellowship.

COMPLIANCE WITH ETHICAL STANDARDS

All animal protocols were approved by the Institutional Animal Care and Use Committee at the University at Buffalo.

REFERENCES

1. Noble RA, Bell N, Blair H, Sikka A, Thomas H, Phillips N, *et al.* Inhibition of monocarboxyate transporter 1 by AZD3965 as a novel therapeutic approach for diffuse large B-cell lymphoma and Burkitt lymphoma. Haematologica. 2017;102(7):1247–57.
2. Polanski R, Hodgkinson CL, Fusi A, Nonaka D, Priest L, Kelly P, *et al.* Activity of the monocarboxylate transporter 1 inhibitor AZD3965 in small cell lung cancer. Clin Cancer Res. 2014;20(4):926–37.
3. Bola BM, Chadwick AL, Michopoulos F, Blount KG, Telfer BA, Williams KJ, *et al.* Inhibition of monocarboxylate transporter-1 (MCT1) by AZD3965 enhances radiosensitivity by reducing lactate transport. Mol Cancer Ther. 2014;13(12):2805–16.
4. Morais-Santos F, Granja S, Miranda-Goncalves V, Moreira AH, Queiros S, Vilaca JL, *et al.* Targeting lactate transport suppresses in vivo breast tumour growth. Oncotarget. 2015;6(22):19177–89.
5. Kong SC, Nohr-Nielsen A, Zeeberg K, Reshkin SJ, Hoffmann EK, Novak I, *et al.* Monocarboxylate transporters MCT1 and MCT4 regulate migration and invasion of pancreatic ductal adenocarcinoma cells. Pancreas. 2016;45(7):1036–47.
6. Morris ME, Felmlee MA. Overview of the proton-coupled MCT (SLC16A) family of transporters: characterization, function and role in the transport of the drug of abuse gamma-hydroxybutyric acid. AAPS J. 2008;10(2):311–21.
7. Halestrap AP, Meredith D. The SLC16 gene family-from monocarboxylate transporters (MCTs) to aromatic amino acid transporters and beyond. Pflugers Arch. 2004;447(5):619–28.
8. Halestrap AP. The monocarboxylate transporter family—structure and functional characterization. IUBMB Life. 2012;64(1):1–9.
9. Halestrap AP, Wilson MC. The monocarboxylate transporter family—role and regulation. IUBMB Life. 2012;64(2):109–19.
10. Pinheiro C, Reis RM, Ricardo S, Longatto-Filho A, Schmitt F, Baltazar F. Expression of monocarboxylate transporters 1, 2, and 4 in human tumours and their association with CD147 and CD44. J Biomed Biotechnol. 2010;2010:427694.
11. Pertega-Gomes N, Vizcaino JR, Miranda-Goncalves V, Pinheiro C, Silva J, Pereira H, *et al.* Monocarboxylate transporter 4 (MCT4) and CD147 overexpression is associated with poor prognosis in prostate cancer. BMC Cancer. 2011;11:312.
12. Fishbein WN, Merezhinskaya N, Foellmer JW. Relative distribution of three major lactate transporters in frozen human tissues and their localization in unfixed skeletal muscle. Muscle Nerve. 2002;26(1):101–12.
13. Ganesan S, Karantza V, Oza J, Toppmeyer D. Triple-negative breast cancers and the human mammary epithelial cell hierarchy. Breast Dis. 2010;32(1–2):49–61.
14. Pinheiro C, Sousa B, Albergaria A, Paredes J, Dufloth R, Vieira D, *et al.* GLUT1 and CAIX expression profiles in breast cancer correlate with adverse prognostic factors and MCT1 overexpression. Histol Histopathol. 2011;26(10):1279–86.
15. Pinheiro C, Albergaria A, Paredes J, Sousa B, Dufloth R, Vieira D, *et al.* Monocarboxylate transporter 1 is up-regulated in basal-like breast carcinoma. Histopathology. 2010;56(7):860–7.
16. Pahlman C, Qi Z, Murray CM, Ferguson D, Bundick RV, Donald DK, *et al.* Immunosuppressive properties of a series of novel inhibitors of the monocarboxylate transporter MCT-1. Transpl Int. 2013;26(1):22–9.
17. Curtis NJ, Mooney L, Hopcroft L, Michopoulos F, Whalley N, Zhong H, *et al.* Pre-clinical pharmacology of AZD3965, a selective inhibitor of MCT1: DLBCL, NHL and Burkitt's lymphoma anti-tumor activity. Oncotarget. 2017;8(41):69219–36.
18. Ovens MJ, Davies AJ, Wilson MC, Murray CM, Halestrap AP. AR-C155858 is a potent inhibitor of monocarboxylate transporters MCT1 and MCT2 that binds to an intracellular site involving transmembrane helices 7-10. Biochem J. 2010;425(3):523–30.
19. Ovens MJ, Manoharan C, Wilson MC, Murray CM, Halestrap AP. The inhibition of monocarboxylate transporter 2 (MCT2) by AR-C155858 is modulated by the associated ancillary protein. Biochem J. 2010;431(2):217–25.
20. Hanson DJ, Nakamura S, Amachi R, Hiasa M, Oda A, Tsuji D, *et al.* Effective impairment of myeloma cells and their progenitors by blockade of monocarboxylate transportation. Oncotarget. 2015;6(32):33568–86.
21. Doherty JR, Yang C, Scott KE, Cameron MD, Fallahi M, Li W, *et al.* Blocking lactate export by inhibiting the Myc target MCT1

disables glycolysis and glutathione synthesis. Cancer Res. 2014;74(3):908–20.
22. Andersen AP, Flinck M, Oernbo EK, Pedersen NB, Viuff BM, Pedersen SF. Roles of acid-extruding ion transporters in regulation of breast cancer cell growth in a 3-dimensional microenvironment. Mol Cancer. 2016;15(1):45.
23. Le Floch R, Chiche J, Marchiq I, Naiken T, Ilc K, Murray CM, *et al.* CD147 subunit of lactate/H+ symporters MCT1 and hypoxia-inducible MCT4 is critical for energetics and growth of glycolytic tumors. Proc Natl Acad Sci U S A. 2011;108(40):16663–8.
24. Tao K, Fang M, Alroy J, Sahagian GG. Imagable 4T1 model for the study of late stage breast cancer. BMC Cancer. 2008;8:228.
25. Bao L, Haque A, Jackson K, Hazari S, Moroz K, Jetly R, *et al.* Increased expression of P-glycoprotein is associated with doxorubicin chemoresistance in the metastatic 4T1 breast cancer model. Am J Pathol. 2011;178(2):838–52.
26. Zhang Y, Zhang N, Hoffman RM, Zhao M. Surgically-induced multi-organ metastasis in an orthotopic syngeneic imageable model of 4T1 murine breast cancer. Anticancer Res. 2015;35(9):4641–6.
27. Kaur P, Nagaraja GM, Zheng H, Gizachew D, Galukande M, Krishnan S, *et al.* A mouse model for triple-negative breast cancer tumor-initiating cells (TNBC-TICs) exhibits similar aggressive phenotype to the human disease. BMC Cancer. 2012;12:120.
28. Sztalmachova M, Gumulec J, Raudenska M, Polanska H, Holubova M, Balvan J, *et al.* Molecular response of 4T1-induced mouse mammary tumours and healthy tissues to zinc treatment. Int J Oncol. 2015;46(4):1810–8.
29. Zhang Y, Schuetz JD, Elmquist WF, Miller DW. Plasma membrane localization of multidrug resistance-associated protein homologs in brain capillary endothelial cells. J Pharmacol Exp Ther. 2004;311(2):449–55.
30. Guan X, Ruszaj D, Morris ME. Development and validation of a liquid chromatography tandem mass spectrometry assay for AZD3965 in mouse plasma and tumor tissue: application to pharmacokinetic and breast tumor xenograft studies. J Pharm Biomed Anal. 2018;155:270–5.
31. Heimburg J, Yan J, Morey S, Glinskii OV, Huxley VH, Wild L, *et al.* Inhibition of spontaneous breast cancer metastasis by anti-Thomsen-Friedenreich antigen monoclonal antibody JAA-F11. Neoplasia. 2006;8(11):939–48.
32. Vijay N, Morse BL, Morris ME. A novel monocarboxylate transporter inhibitor as a potential treatment strategy for gamma-hydroxybutyric acid overdose. Pharm Res. 2015;32(6):1894–906.
33. Wang Q, Lu Y, Morris ME. Monocarboxylate transporter (MCT) mediates the transport of gamma-hydroxybutyrate in human kidney HK-2 cells. Pharm Res. 2007;24(6):1067–78.
34. Lanari C, Luthy I, Lamb CA, Fabris V, Pagano E, Helguero LA, *et al.* Five novel hormone-responsive cell lines derived from murine mammary ductal carcinomas: in vivo and in vitro effects of estrogens and progestins. Cancer Res. 2001;61(1):293–302.
35. Payen VL, Hsu MY, Radecke KS, Wyart E, Vazeille T, Bouzin C, *et al.* Monocarboxylate transporter MCT1 promotes tumor metastasis independently of its activity as a lactate transporter. Cancer Res. 2017;77(20):5591–601.
36. Bhattacharya I, Boje KM. GHB (gamma-hydroxybutyrate) carrier-mediated transport across the blood-brain barrier. J Pharmacol Exp Ther. 2004;311(1):92–8.
37. Roiko SA, Felmlee MA, Morris ME. Brain uptake of the drug of abuse gamma-hydroxybutyric acid in rats. Drug Metab Dispos. 2012;40(1):212–8.
38. Vijay N, Morris ME. Role of monocarboxylate transporters in drug delivery to the brain. Curr Pharm Des. 2014;20(10):1487–98.
39. Gerhart DZ, Enerson BE, Zhdankina OY, Leino RL, Drewes LR. Expression of monocarboxylate transporter MCT1 by brain endothelium and glia in adult and suckling rats. Am J Phys. 1997;273(1 Pt 1):E207–13.